Supplemental Information

Supplemental Information I – Model Schematic:

Figure S1 shows the basic elements of our ZIKV model. Transition rates between states, along with ranges for these parameters, can be found in Table S1 of Supplemental Information II.

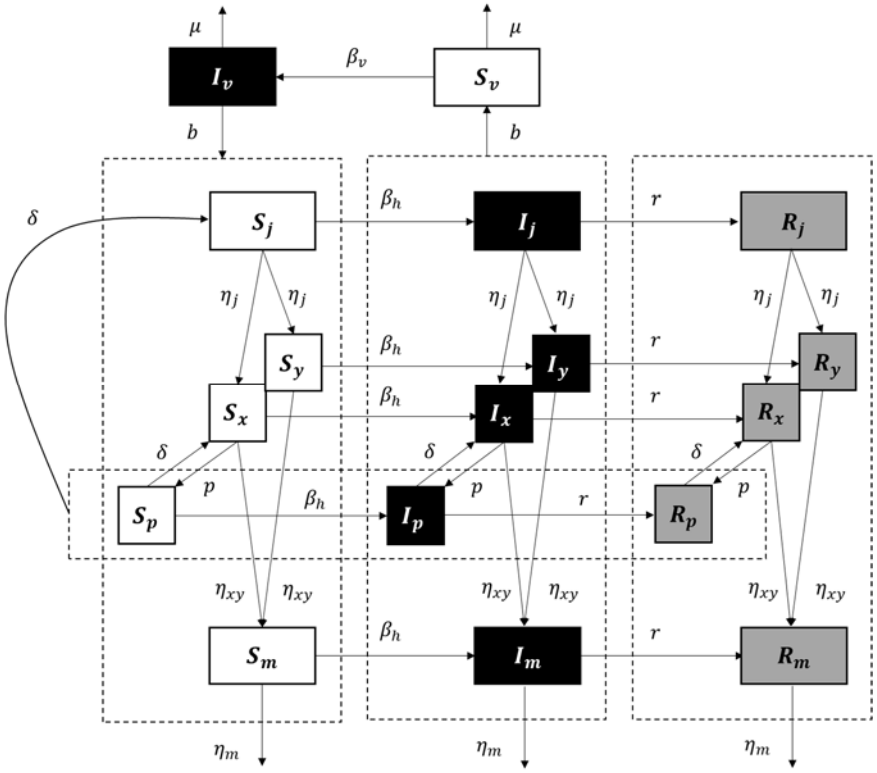

Figure S1 Schematic illustrating transitions between the different compartments in our model. The human host population can be susceptible (white), infected (black) or recovered (grey), while the vector population is either susceptible (white) or infected (black). For the human population, subscripts indicate the following: *j* for children, *x* for reproductive females that are not pregnant, *p* for reproductive females that are pregnant, *y* for reproductive males and *m* for post-reproductive adults. Dashed boxes demark classes with shared transitions.

Supplemental Information II – Model Parameterization:

Human parameters are well defined based on known demographic information (see Table S1). For mosquito parameters, we use values previously determined from analysis of DENV models. We believe that this is valid, since DENV is also spread by *Aedes* mosquitoes, and *Ae. aegypti* in particular. For disease parameters (the probability of mosquito to human transmission, β_h, the probability of human to mosquito transmission, β_v, and the human infectious period, $1/r$), we again select ranges based on DENV. For the human infectious period, the parameter range for DENV is consistent with preliminary estimates from recent ZIKV outbreaks[1]. For transmission probabilities, DENV parameter ranges are broad. Consequently, we use ZIKV seroprevalence rates to identify ranges for these parameters that are more likely (see below). These narrower ranges are then used for scenario analysis throughout the main text.

Table S1 Parameter Definitions and Ranges*

Parameter	Definition	Range	Ref.
η_j^{-1}	human age at first reproduction	15-25 years	2
η_{xy}^{-1}	human reproductive period	20-25 years	3
η_m^{-1}	human lifespan following reproduction	20-30 years	4
p/η_{xy}	children per female	2	-
δ^{-1}	Gestation	37-40 weeks	-
N_h	human population size**	5000-15000 area^{-1}	5
A	mosquito recruitment	400-5000 day^{-1}area^{-1}	5,6
μ^{-1}	mosquito life expectancy	4-50 days	5,6
b	mosquito biting rate	0.3-1 day^{-1}	5,6
β_h	probability of mosquito to human transmission	0.1-0.75	5,6
β_v	probability of human to mosquito transmission	0.5-1	5,6
r^{-1}	human infectious period	3-14 days	5,6

* human population size and mosquito recruitment are defined for an arbitrary unit area; the important parameter is the ratio of number of mosquitoes ($N_v \longrightarrow A/\mu$) to humans ($N_h$). In reality, this is highly variable, depending on season, rainfall, habitat and geographical location. The average parameter values in Table S1 give a ratio of N_v: $N_h = 7.29$, which is reasonable based on pupal density estimates from a study in Rio de Janeiro[7] combined with the fact that the adult lifespan of *Ae. aegypti* is 2-4 weeks versus the approximately 2 day pupal stage.

**We set $p/\eta_{xy} = 2$ to ensure that the human population size remains fixed at a constant N_h. This essentially means that each couple has, on average, two children. We choose a fixed population because this makes it easier to understand system behavior, which would otherwise be complicated by an underlying change in population size. We realize, however, that most countries with ZIKV outbreaks have growing populations. We explore model behavior for a growing population in Supplemental Information V.

Dengue-Based Parameterization: First, we consider predictions based on average values in Table S1. For this parameterization to be accurate, the probabilities of DENV transmission between humans and mosquitoes must be comparable to the corresponding probabilities for ZIKV. Although both DENV and ZIKV are flaviviruses, there is no guarantee that transmission probabilities will be similar for the two diseases. In general, we find that using average parameter values based on DENV studies yields high seroprevalence rates as compared to estimates based on studies where ZIKV is endemic. However, this could reflect differences (temperature, vector species, vector abundances, etc.) between regions where DENV modeling is focused and regions where ZIKV seroprevalence has been measured, rather than true differences between disease transmission probabilities (see below). Figure S2e shows predicted ZIKV dynamics under the assumption that ZIKV transmission is similar to DENV transmission.

Seroprevalence Based Parameterization: Our second parameterization scheme depends on fitting model predicted seroprevalence rates from endemic systems to those observed in regions of Africa, where ZIKV has existed for many years. For this parameterization scheme to be correct, all parameters except transmission rates must be comparable between regions where DENV modeling is focused and regions where ZIKV seroprevalence has been measured. If, for example, mosquito density is lower in the regions of Africa where ZIKV seroprevalence rates have been measured, then using artificially high estimates of mosquito density based on DENV modeling could cause us to underestimate disease transmission probabilities. In essence, we would be forcing seroprevalence rates in the Americas to be equal to seroprevalence rates in Africa, even though this should not be the case based on differences in mosquito populations. Ideally, transmission rates should be measured independently of seroprevalence data, based on laboratory studies. However, since these measurements do not yet exist, we use fitted seroprevalence rates to help inform our range of most likely transmission probabilities, admitting that this is an imperfect estimate.

Because seroprevalence should depend on age, at least under the condition of endemic ZIKV, we focus on a study that collected age-structured seroprevalence data. Specifically we use Geser, et al. [8], focusing on

the Malindi District, where *Aedes* species are prevalent. Fixing human and mosquito parameters, as well as the human infectious period, at the average values from Table S1 (notice that this gives the human infectious period at 5 days, which is consistent with ZIKV data[1]), we note that disease dynamics are only sensitive to the product of the two transmission rates (see Figure S2). Consequently, we set $\beta_h = 0.5$ and tune β_v to match seroprevalence data from the Malindi District. For this, we consider seroprevalence rates after 500 years of disease spread, which is sufficient for ZIKV to reach an endemic (i.e. equilibrium) state. We then determine β_v values by separately fitting seroprevalence data for juveniles, reproductive adults, post-reproductive adults and the overall community (for this last case, we use an age-adjusted seroprevalence rate based on the age-structure in our modelled population). Results are shown in Table S2, which includes predicted population-wide seroprevalence rates for the first year of a ZIKV outbreak (as opposed to endemic spread).

Table S2 Estimated transmission rates based on seroprevalence data*

Fitted Class	Average Seroprevalence[8]	β_v ($\beta_v \cdot \beta_h$)	Year 1 Seroprevalence
juveniles	12.9%	0.0885 (0.0442)	36.5%
reproductive adults	63.6%	0.170 (0.0848)	85.6%
post-reproductive adults	87.6%	0.225 (0.112)	92.4%
overall	57.6%	0.153 (0.0763)	81.9%

*for the juvenile class, we use all age classes below 14 years of age, as well as half of the 15-19 year age class. For the reproductive class, we use half of the 15-19 year age class, and all age classes between 20-39 years of age. For the post-reproductive class, we use all age classes above 40 years of age.

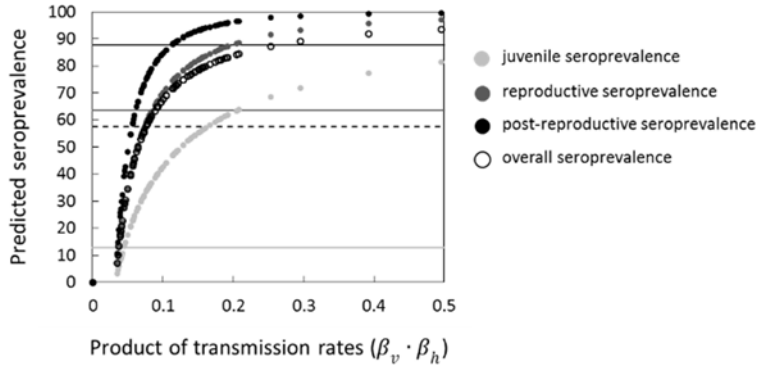

Figure S3 Model predicted seroprevalence rates for juveniles (light grey, solid circles), reproductive adults (dark grey, solid circles), post-reproductive adults (black, solid circles), and the overall population (open circles). Horizontal lines show seroprevalence rates for juveniles (light grey, solid), reproductive adults (dark grey, solid), post-reproductive adults (black, solid), and the overall community (black, dashed) based on empirical study in the Malindi District.

Figure S3 shows predicted disease dynamics corresponding to each of the above fits. Notice that most parameterizations predict an outbreak duration of ~5 months in any given location, which is consistent with reports from Polynesia and Micronesia[9]. In the main paper, we use fits based on juvenile seroprevalence as our low estimate (i.e., 'low transmission' scenario), fits based on average DENV parameters as our high estimate (i.e., 'high transmission' scenario), and fits based on the overall (age-adjusted) population-wide seroprevalence as our intermediate estimate (i.e., 'intermediate transmission' scenario). Notice that our intermediate transmission scenario gives a predicted population-wide coverage of 80% following the first year of a ZIKV outbreak, which is consistent with reports from Micronesia[9], though slightly above reports from Yap Island[10] and French Polynesia[9].

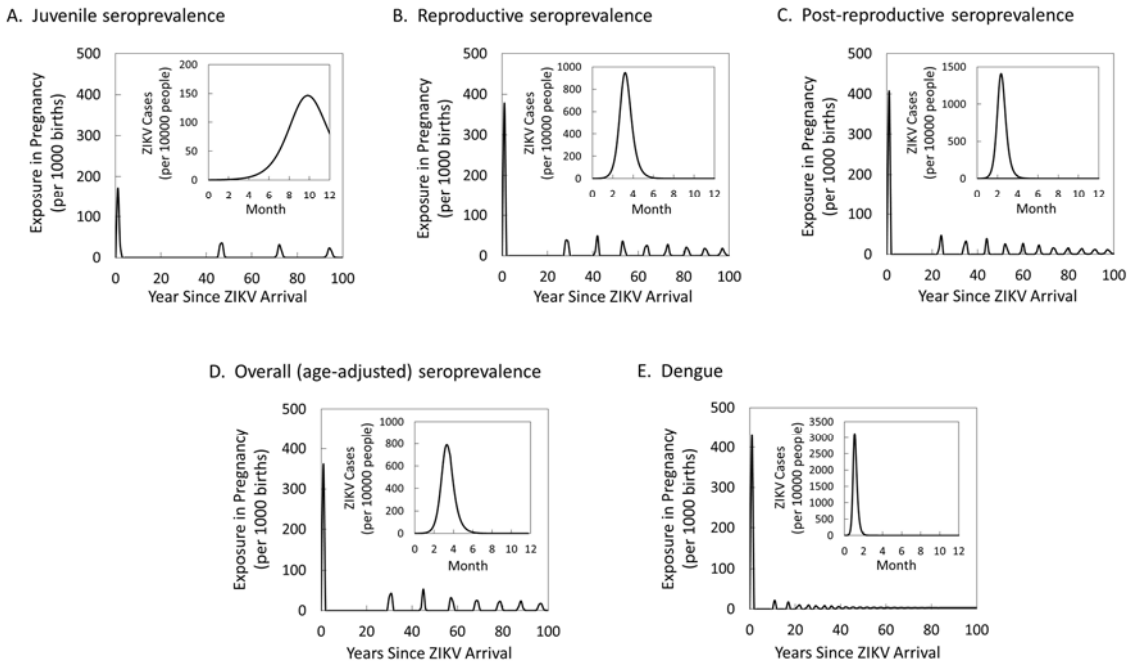

Figure S3 Predicted number of pregnantwomen who experience a ZIKV infection as a function of the number of years since ZIKV was first introduced. Insets show the total number of ZIKV cases during the first year of the outbreak. Panels are for transmission rates fitted (a) based on juvenile seroprevalence rates ($\beta_v \cdot \beta_h = 0.0442$); (b) based on reproductive-aged seroprevalence rates ($\beta_v \cdot \beta_h = 0.0848$); (c) based on post-reproductive aged seroprevalence rates ($\beta_v \cdot \beta_h = 0.112$); (d) based on the overall population seroprevalence rate ($\beta_v \cdot \beta_h = 0.0763$); and (e) based on average DENV parameters ($\beta_v \cdot \beta_h = 0.319$).

Supplemental Information III

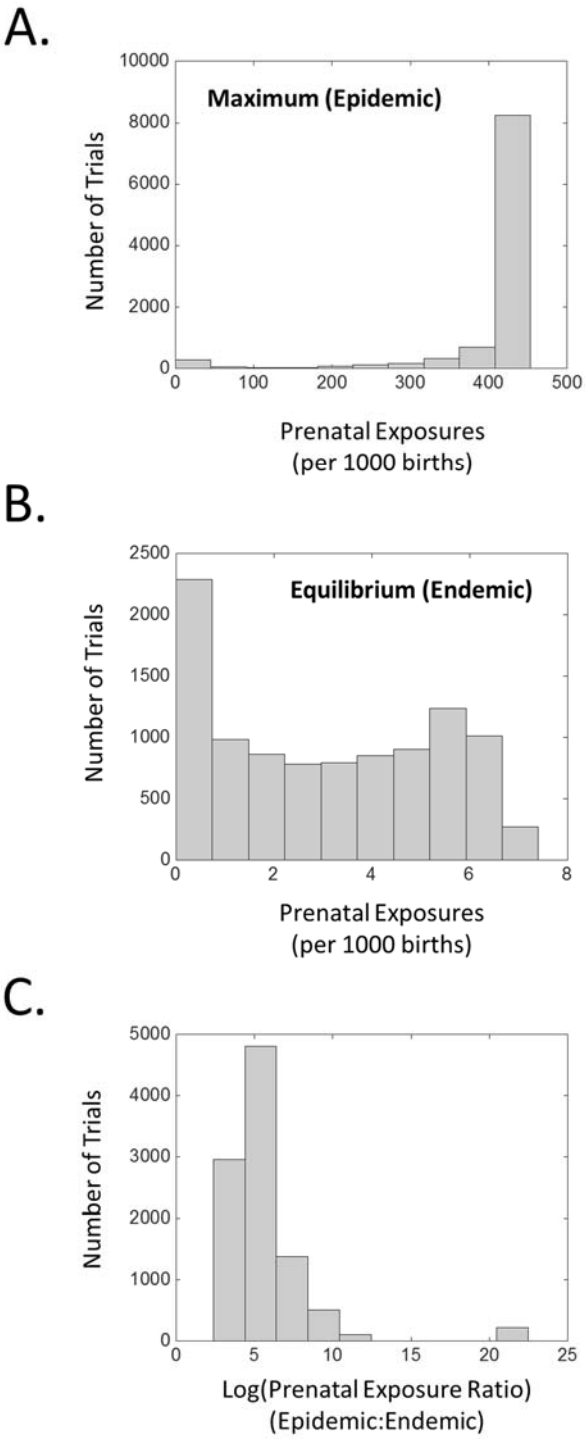

Figure S4 shows histograms summarizing results from our Latin Hypercube Sampling (LHS) analysis. Notice that the majority of scenarios predict maximum prenatal exposure rates >400 per 1000 births. By contrast, equilibrium scenarios predict prenatal exposure rates <10 per 1000 births. The dramatic reduction from epidemic scenarios (shortly after ZIKV is introduced into a region) to endemic scenarios (after the virus has been circulating for long periods of time) is further highlighted by the ratio of maximum prenatal exposure rate to equilibrium prenatal exposure rate, which shows that most systems exhibit a ~150-fold decrease in going from epidemic to endemic conditions.

Figure S4 Histograms showing the number of LHS trials with given (A) maximum prenatal exposure rates (B) equilibrium prenatal exposure rates and (C) maximum:equilibrium prenatal exposure rates. LHS sampling was over the ranges in Table S1, but assuming the following restrictions to ensure monotonicity: $b \in (0.4, 1)$, $A \in (1000, 5000)$ and $\beta_h \in (0.15, 0.75)$.

Supplemental Information IV:

To explore the incidence of microcephaly in the case that high risk is only associated with ZIKV infection during the early stages of pregnancy, we divide the pregnancy class in equations (1-6) into two separate stages, as follows:

Pre-reproductive females and males:

$$\frac{dS_j}{dt} = \overbrace{\delta_2\left(S_{p,2} + I_{p,2} + R_{p,2}\right)}^{birth} - \overbrace{\eta_j S_j}^{maturation} - \overbrace{\frac{\beta_h b}{N_h} S_j I_v}^{infection} \quad \text{(S4.1)}$$

Reproductive females (*not pregnant*):

$$\frac{dS_x}{dt} = \overbrace{\frac{\eta_j}{2} S_j}^{maturation} - \overbrace{\eta_{xy} S_x}^{maturation} - \overbrace{p S_x}^{pregnancy} + \overbrace{\delta_2 S_{p,2}}^{delivery} - \overbrace{\frac{\beta_h b}{N_h} S_x I_v}^{infection} \quad \text{(S4.2.a)}$$

$$\frac{dI_x}{dt} = \overbrace{\frac{\eta_j}{2} I_x}^{maturation} - \overbrace{\eta_{xy} I_x}^{maturation} - \overbrace{p I_x}^{pregnancy} + \overbrace{\delta_2 I_{p,2}}^{delivery} + \overbrace{\frac{\beta_h b}{N_h} S_x I_v}^{infection} - \overbrace{r I_x}^{recovery} \quad \text{(S4.2.b)}$$

$$\frac{dR_x}{dt} = \overbrace{\frac{\eta_j}{2} R_j}^{maturation} - \overbrace{\eta_{xy} R_x}^{maturation} - \overbrace{p R_x}^{pregnancy} + \overbrace{\delta_2 R_{p,2}}^{delivery} + \overbrace{r I_x}^{recovery} \quad \text{(S4.2.c)}$$

Reproductive females (*pregnant, at risk*)*:*

$$\frac{dS_{p,1}}{dt} = \overbrace{p S_x}^{pregnancy} - \overbrace{\delta_1 S_{p,1}}^{leaving\ risk\ stage} - \overbrace{\frac{\beta_h b}{N_h} S_{p,1} I_v}^{infection} \quad \text{(S4.3.a)}$$

$$\frac{dI_{p,1}}{dt} = \overbrace{p I_x}^{pregnancy} - \overbrace{\delta_1 I_{p,1}}^{leaving\ risk\ stage} + \overbrace{\frac{\beta_h b}{N_h} S_{p,1} I_v}^{infection} - \overbrace{r I_{p,1}}^{recovery} \quad \text{(S4.3.b)}$$

$$\frac{dR_{p,1}}{dt} = \overbrace{p R_x}^{pregnancy} - \overbrace{\delta_1 R_{p,1}}^{leaving\ risk\ stage} + \overbrace{r I_{p,1}}^{recovery} \quad \text{(S4.3.c)}$$

Reproductive females (*pregnant, not at risk*)*:*

$$\frac{dS_{p,2}}{dt} = \overbrace{\delta_1 S_{p,1}}^{leaving\ risk\ stage} - \overbrace{\frac{\beta_h b}{N_h} S_{p,2} I_v}^{infection} - \overbrace{\delta_2 S_{p,2}}^{delivery} \quad \text{(S4.3.a)}$$

$$\frac{dI_{p,2}}{dt} = \overbrace{\delta_1 I_{p,1}}^{\substack{leaving\\risk\ stage}} + \overbrace{\frac{\beta_h b}{N_h} S_{p,2} I_v}^{infection} - \overbrace{rI_{p,2}}^{recovery} - \overbrace{\delta_2 I_{p,2}}^{delivery} \quad \text{(S4.3.b)}$$

$$\frac{dR_{p,2}}{dt} = \overbrace{\delta_1 R_{p,1}}^{\substack{leaving\\risk\ stage}} + \overbrace{rI_{p,2}}^{recovery} - \overbrace{\delta_2 R_{p,2}}^{delivery} \quad \text{(S4.3.c)}$$

Mosquitoes:

$$\frac{dS_v}{dt} = A - \overbrace{\mu S_v}^{death} - \overbrace{\frac{\beta_v b}{N_h} S_v \left(I_j + I_x + I_{p,1} + I_{p,2} + I_y + I_m\right)}^{infection} \quad \text{(S4.4.a)}$$

$$\frac{dI_v}{dt} = - \overbrace{\mu I_v}^{death} + \overbrace{\frac{\beta_v b}{N_h} S_v \left(I_j + I_x + I_{p,1} + I_{p,2} + I_y + I_m\right)}^{infection} \quad \text{(S4.4.b)}$$

where we have only shown those equations that are modified, and where the total length of the gestation period is given by $1/\delta_1 + 1/\delta_2$. Figure S5 shows how the length of the high risk period affects both the maximum (epidemic) and equilibrium (endemic) rates of high risk ZIKV exposures for the high transmission scenario. As expected, shorter high risk periods result in lower numbers of high risk exposures, with a nearly linear relationship between the length of the high risk period and the exposure rate. Despite this, we see that even if high risk is only associated with ZIKV infection during the first trimester, over 10% of pregnant women will experience a high risk ZIKV infection during an epidemic. Under endemic conditions, the risk is closer to 0.1%.

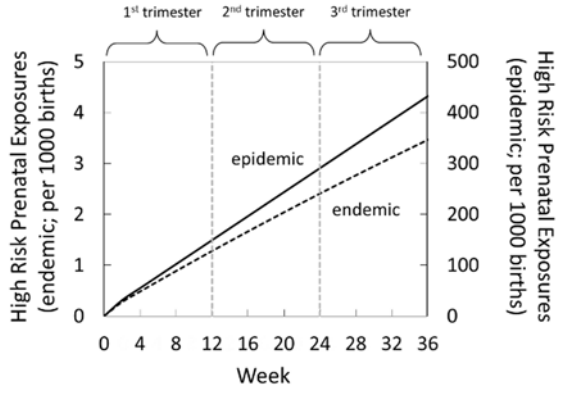

Figure S5 The number of high risk prenatal exposures as a function of the length of the high risk period for systems where ZIKV has been newly introduced (epidemic, solid) and systems where ZIKV has been circulating for many years (endemic, dashed). We assume average values for all parameters (see Table S1) except the gestation period, which is broken into a high risk period and a low risk period, always totaling 9 months. Note that the y-axes for epidemic and endemic dynamics differ by 100-fold.

Supplemental Information V:

To explore the effect of population growth, we consider prenatal exposures at long time-points ($t = 500$) for growing populations (note that growing populations will not reach an equilibrium). For these scenarios, we use the high transmission scenario, begin with $N_h = 10000$, and an age-distribution consistent with an equilibrium population. We then allow the population to grow ($p = 2.1\eta_{xy}$), considering similar dependencies as in Figure 4 of the main text. Results are shown in Figure S6. From this figure, it is clear that the same qualitative trends in prenatal exposures that we observed in steady-state populations also hold in systems with growing populations.

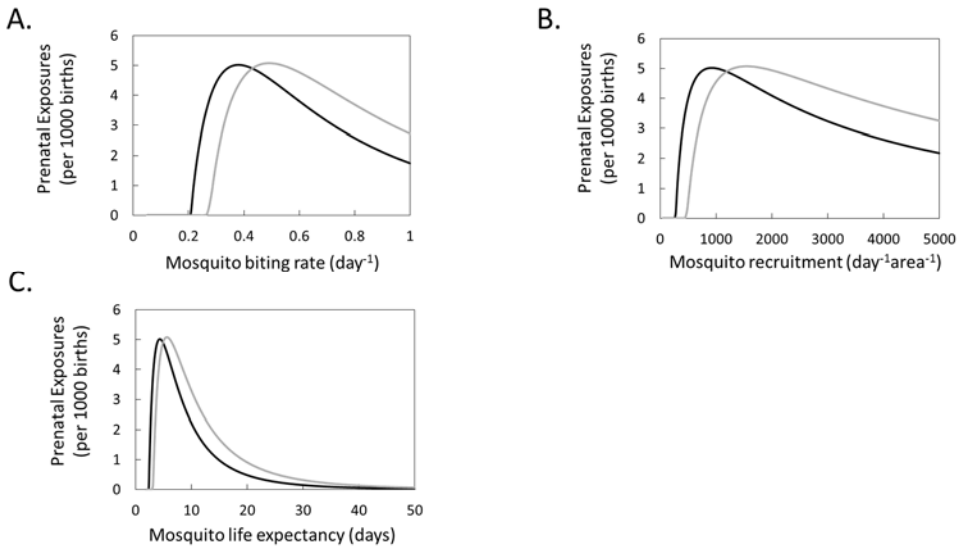

Figure S6 Number of women who experience an active ZIKV infection at any point during pregnancy as a function of (A) mosquito biting rates, (B) mosquito recruitment rates and (C) mosquito life expectancy in a region with endemic disease (i.e., a system at equilibrium) for a population of constant size (black) and an increasing population (bgrey). In each panel, we assume average values for all parameters except the one being varied (see Table S1).

Supplementary Information VI

Figure S7 shows monotonicity plots for endemic prenatal exposures against each of the 11 variables in our LHS matrix. From this Figure, we see that b, A, and β_h are obviously non-monotonic at low values. Therefore, to perform PRCC analysis, we restrict the ranges of these parameters to $b \in (0.4, 1)$, $A \in (1000, 5000)$ and $\beta_h \in (0.15, 0.75)$ respectively. This means that LHS results only apply under the assumption that mosquito biting rates, mosquito recruitment and mosquito-to-human transmission are reasonably high (in practice, high enough to prevent $R_0 \approx 1$). Restricting the ranges of mosquito biting rates, mosquito recruitment rates and mosquito-to-human transmission removes the slight non-monotonicity observed in η_{xy} and μ, so we use the full range for these two parameters.

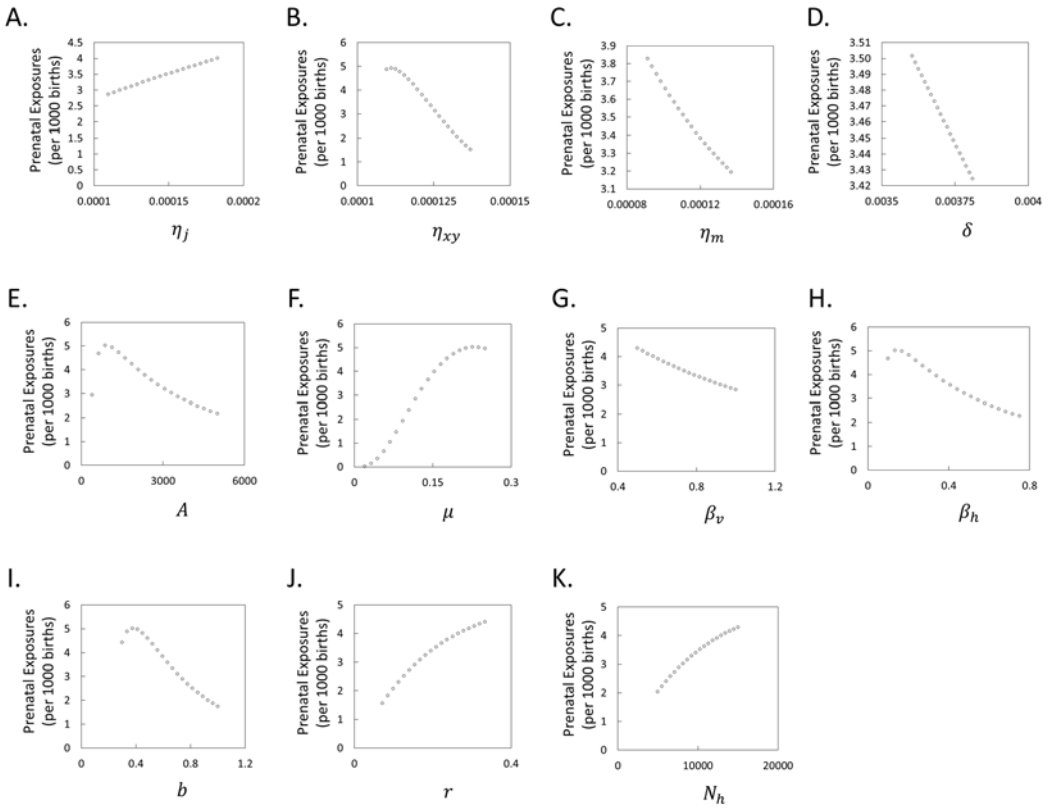

Figure S7 Monotonicity plots for endemic prenatal exposures against the 11 variables in our LHS analysis. In each panel, we assume average values for all parameters except the one being varied (see Table S1).

References for Supplemental Information

1 Mallet, H. Bilan de l'épidémie à virus zika en Polynésie française, 2013-2014. *Bises (Bulletin d'Information sanitaires, épidémiologiques et statistiques)*, 1-5 (2015).

2 Bongaarts, J. & Blanc, A. K. Estimating the current mean age of mothers at the birth of their first child from household surveys. *Population health metrics* **13**, 1 (2015).

3 Schoenaker, D. A., Jackson, C. A., Rowlands, J. V. & Mishra, G. D. Socioeconomic position, lifestyle factors and age at natural menopause: a systematic review and meta-analyses of studies across six continents. *International journal of epidemiology* **43**, 1542-1562 (2014).

4 (World Health Organization, WHO. 2015, Geneva, Switzerland, 2015).

5 Esteva, L. & Vargas, C. Analysis of a dengue disease transmission model. *Mathematical biosciences* **150**, 131-151 (1998).

6 Andraud, M., Hens, N., Marais, C. & Beutels, P. Dynamic epidemiological models for dengue transmission: a systematic review of structural approaches. *PloS one* **7**, e49085 (2012).

7 Maciel-de-Freitas, R., Marques, W. A., Peres, R. C., Cunha, S. P. & Lourenço-de-Oliveira, R. Variation in Aedes aegypti (Diptera: Culicidae) container productivity in a slum and a suburban district of Rio de Janeiro during dry and wet seasons. *Memórias do Instituto Oswaldo Cruz* **102**, 489-496 (2007).

8 Geser, A., Henderson, B. E. & Christensen, S. A multipurpose serological survey in Kenya: 2. Results of arbovirus serological tests. *Bulletin of the World Health Organization* **43**, 539 (1970).

9 Torjesen, I. Zika virus outbreaks prompt warnings to pregnant women. *BMJ* **352**, i500 (2016).

10 Duffy, M. R. *et al.* Zika virus outbreak on Yap Island, federated states of Micronesia. *New England Journal of Medicine* **360**, 2536-2543 (2009).